

## Lumbar Loads in Low to Moderate Speed Rear Impacts

2010-01-0141

Published  
04/12/2010

Deanna Gates, Amanda Bridges, Torrence D. J. Welch, Tack Lam, Irving Scher and Gary Yamaguchi  
Exponent Failure Analysis

Copyright © 2010 SAE International

### ABSTRACT

Although most of the research on vehicular rear impacts has focused on the neck, there is increasing current concern about the lumbar spine. Spinal bending superimposed with sudden spinal compression has been suggested as a mechanism of creating acute herniations on the rare occasion in which low back pain associated with an intervertebral disc herniation was reported. During automotive rear-impacts, the vehicle accelerations are directed anteriorly, and the seat backs deflect posteriorly. In vehicle seats equipped with floor-mounted seatbelt restraints, the pelvis is restrained by the seatback and seatbelt, while the torso ramps upward and rearward on the seatback during the rearward motion, producing tension in the lumbar spine. However, in an all-belts-to-seat arrangement, the lumbar spines may experience overall compressive and bending loads. With either seatbelt arrangement, the spine might experience some transient bending and compression, which could be consistent with the proposed mechanism of acute disc herniation.

This paper explored spinal bending and loading during rear impacts with changes of velocity (delta Vs) of 2.2, 3.6, 5.4, and 6.7 m/s (5, 8, 12, 15 mph), using Hybrid III and BioRID II anthropomorphic test devices (ATDs). Male 50<sup>th</sup>-percentile ATDs of both types were seated side-by-side on a pneumatic test sled and restrained with 3-point belts. One test at each speed was run using floor mounted restraints (Ford Taurus 2002-2003), and one test each was run at 2.2 m/s and 5.4 m/s delta Vs using an all-belts-to-seat configuration (2001 Chevrolet Suburban). Lumbar forces and moments were measured using the two types of ATDs. High speed videos were used to grossly assess ATD motion patterns. The overall results were compared to the literature to determine if the ATD lumbar spines in our tests experienced loads compatible

with the creation of acute disc herniations and protrusions during low to moderate speed rear impacts.

### INTRODUCTION

Although most of the research on vehicular rear impacts has focused on the neck, there is increasing current concern about the lumbar spine [1, 2]. Historically, there has been a lack of focus on the behavior of the lumbar spine during rear impacts because of the perception that a properly designed and correctly used seat back should protect the lower spine from injury [3]. This perception is reinforced by past human volunteer experiments that showed human tolerance to rear impacts in properly supported seats to be around 28 to 42 Gs, levels of acceleration much higher than those encountered in common low speed rear impacts [4]. In a review of 364 low speed rear impacts using human volunteers, only one complaint of a “slight ache in the lumbar region” was reported by a subject who was leaning forward at impact [5]. The prevalence of low back pain associated with a cervical whiplash syndrome was reported to be 25 % [2].

The mechanism to create a lumbar spine injury in a rear impact is unclear. In a radiographic study of a human lumbar spine in a driving posture, it was reported that the arrangement of the lumbar vertebrae in a normal driving posture was similar to that when the human subject voluntarily flexed his spine [1]. The lower back in a driving posture approximated a straight line that was nearly parallel to the seat back axis [1]. The anterior disc thickness was noted to be a sensitive indicator of posture while the posterior disc thickness was not [1]. Consequently, it was concluded that a tension injury to the posterior spinal elements resulting from a low velocity rear end collision would be unlikely [1].

One cause of low back pain is an acute intervertebral disc herniation [6]. An intervertebral disc is an avascular structure that provides separation and permits movement between two adjacent vertebrae [7]. Discs are composed of two primary components: the annulus fibrosus (annulus) and the nucleus pulposus (nucleus). The nucleus is a jelly-like substance at the center of the disc that has the consistency of toothpaste [8, 9]. The annulus is a fibrous, multilayered circumferential structure, similar in construction to an automobile tire with multiple plies. Like the plies of a tire, the fibers in a disc are oriented differently in the various layers, and each layer resists loads along its fiber axis [9]. This composite mechanical arrangement, with reinforcing fibers oriented in different directions in the adjacent layers, makes the disc very resistant to physiological loads in a most efficient manner [9]. Because the alternating layers resist loads in different directions, it is practically impossible to tear the annulus of a healthy disc all the way through during a single traumatic loading event.

Previous studies have examined the relationship between loading and disc damage. Most of these studies have examined functional spinal units (a vertebra-disc-vertebra segment) of the lumbar spine using compression, anterior-posterior shear, sagittal plane bending moments, and spinal torsion. Within the physiologic range of motion, *in vitro* studies have only been able to reproduce traumatic herniation through a combination of compression and flexion [10]. These authors also suggested that lateral bending can act as a catalyst. Bending alone does not appear to be capable of producing a herniation, even though bending does generate tension on one side of the annulus and compression on the other. Bending and sudden compression appears to be harmful because the bending first stresses all of the annular rings on one side of the disc in tension, and then the sudden compression causes a rapid increase of fluid pressure exerted laterally upon the already stretched fibers on the tension side.

Compression is resisted by both the intervertebral disc and the facet joints [11]. The portion of the compressive load resisted by the disc is transferred to the nucleus, which in turn exerts a high fluid pressure against the walls of the annulus [9]. If the annulus has a tear or other defect, the hydrostatic pressure causes the nuclear material to migrate through the defect [12]. A localized displacement of the nucleus beyond the intervertebral disc space, called a herniation, can occur radially outward, as well as through the vertebral endplates above and below the disc. Compressive loading at slow and high speeds creates fractures in the vertebral endplates and not failure in the disc [13]. Sudden or traumatic disc herniation has been produced in spinal test specimens when the vertebrae were first placed simultaneously in hyperflexion and lateral bending, and then suddenly loaded by a compressive force [12]. However, compressive loads in the physiologic range were not noted to produce disc herniations even when the annular fibers were surgically cut to within 1

mm of the outer edges of the disc [14]. The latter study concluded that an extensive disruption to the internal annular fibers was insufficient to enable the discs to herniate under normal physiologic loads.

In summary, disc herniations are described in the literature primarily as a fatigue injury. Adams and Hutton [7] describe first fatiguing the discs by cyclic loading disc specimens 40 times per minute at loads between 1.5 and 6.0 kN. 11 of 41 specimens failed prior to the end of the 4 hours of cyclic loading. 20 of the disc specimens were then compressed a single time to attempt to cause disc prolapse. Three of the 20 specimens tested this way caused the disc to prolapse. The forces to produce these such herniations were 5.0, 5.8, and 6.8 kN.

ATDs have been used by the automotive industry to assess the likelihood of injury in motor vehicle accidents. The Hybrid III 50<sup>th</sup>-percentile male ATD was developed in 1973 and is currently used in Federal Motor Vehicle Safety Standard (FMVSS) 208 testing for occupant crash protection. The Biofidelic Rear Impact Dummy (BioRID) II 50<sup>th</sup>-percentile male ATD was recently developed to measure responses specifically in low speed rear impact tests and has been validated against the kinematics of human volunteers in low speed crash tests [15, 16]. The BioRID II uses many of the same components found in the Hybrid III, including arm and leg assemblies, but the BioRID II has modified Hybrid III pelvis and head assemblies [17]. Component sections of both ATDs are identical in weight and dimension [17].

The BioRID II spine assembly consists of seven cervical, twelve thoracic, and five lumbar “vertebrae.” Other than T1, all vertebrae are made from durable plastic and are connected with pins at each joint. The pin joints keep the vertebrae positioned relative to each other and allows each vertebra to rotate primarily in the sagittal plane. The pins somewhat like mechanical substitutes for facet joints in the human spine, except that they do not allow for rotations about the axis of the spine (as in the thoracic spine [18]) or coupled axial rotations and lateral bending (as in the cervical spine [9]). Polyurethane rubber bumper pads are attached to the top of each vertebra to simulate compression resistance during flexion and extension. The pin joints take up the remainder of the compression load. Three interface regions (occipital, T1, and pelvis) are made of aluminum. The BioRID II also contains tensioning devices, mounted in the torso, which act as dampening and spring-loaded, passive muscle substitutes. The BioRID II 6-channel lumbar spine load cell inserts at the L5 location in a horizontal orientation atop a modified Hybrid III pelvis (Figure 1) [17].

<figure 1 here>

The Hybrid III lumbar spine differs from that of the BioRID II. The Hybrid III lumbar spine is a curved, continuous piece of molded polyacrylate material with two lumbar cables that run through the spinal cavity to provide lateral stabilization [19]. In contrast to the lordotic curvature (concave posteriorly) of human and BioRID II lumbar spines, the Hybrid III lumbar spine is curved forward in a kyphotic curvature (concave anteriorly). The kyphotic curvature of the Hybrid III lumbar spine adds “humanlike slouch” to the seated ATD [19]. The Hybrid III lumbar spine attaches to the thoracic spine via a steel thoracic spine assembly, and it attaches to the pelvis via a steel lumbar-to-pelvis adaptor. A 3-channel lumbar spine load cell inserts between the lumbar and pelvis sections of the Hybrid III. This sensor mounts to the lumbar section that is manufactured at a 22° angle (posteriorly downward) (Figure 1) [17].

The purpose of the current study was to ascertain whether the conditions necessary for producing traumatic lumbar disc herniations are evident during low and moderate speed rear end collisions. Both Hybrid III and BioRID II lumbar spinal loads were measured in multiple sled tests simulating rear-end crashes over a range of velocities and accelerations. The loads measured using the two ATD types were compared and related to the loads and forces required to produce acute lumbar disc herniations.

## METHODS

To examine the effect of a rear impact on lumbar loads, a series of tests were conducted using ATDs in different seat configurations at different crash severities (Table 1). Sled tests simulating rear impact were conducted using a 170-ft rail, a pneumatic acceleration system, and a programmable wire-bending decelerator [20].

<table 1 here>

## SEAT CONFIGURATIONS

For the first set of tests (A-D), manual actuation front bucket seats from a 2001-2003 model year Ford Taurus were rigidly secured to the sled. Prior to testing, the seats were visually inspected and showed no deformities. The condition of the three vehicles from which the seats were taken was similar, with odometer readings ranging from 50,724 to 85,396 miles. The three-point continuous loop seatbelt restraint system and corresponding anchor points used in each test matched the dimensions of the source vehicle. These seats were tested at delta Vs of 2.2, 3.6, 5.4, 6.7 m/s (5, 8, 10, and 12 mph). Seats were replaced after Tests B and C due to post-test deformation.

For the next set of tests (E-F), front seats from a 2001 Chevrolet Suburban were rigidly secured to the sled. The source vehicle had an odometer reading of 87,289 miles, and

no deformation of the seats was noted prior to testing. The seats contained an integrated restraint system (all-belts-to-seats), in which the entire seat-belt restraint system was mounted directly to the seat, rather than to the floor or B-pillar. These seats were tested at delta Vs of 2.2 and 5.4 m/s (5 and 12 mph).

## ANTHROPOMORPHIC TEST DEVICE CONFIGURATION

A 50<sup>th</sup>-percentile Hybrid III ATD was placed in the passenger's seat, and a BioRID II ATD was placed in the driver's seat. Both ATDs were placed in a forward-facing position, positioned in accordance with FMVSS 208, and secured using the three-point restraint system (Figure 2). The seating positions were consistent across all speeds and seat-types.

<figure 2 here>

## INSTRUMENTATION

The impact velocity of the sled was measured using a velocity trap, and the sled acceleration was measured using sled-mounted accelerometers. High-speed video was recorded at 500 frames per second using on-board digital cameras on the right and left sides of the sled (Figure 2). Lumbar loads for the Hybrid III were measured using a tri-axial load cell to quantify anterior/posterior shear force ( $F_x$ ), compression/tension force ( $F_z$ ), and flexion/extension moments ( $M_y$ ). Lumbar loads for the BioRID II were measured using a six-axis load cell to measure anterior/posterior shear force ( $F_x$ ), left/right lateral shear force ( $F_y$ ), compression/tension force ( $F_z$ ), moment about the anterior/posterior axis ( $M_x$ ), flexion/extension moment ( $M_y$ ), and torsional moment ( $M_z$ ).

## DATA ANALYSIS

Each channel of data was recorded at 10,000 samples per second and was passed through a 2,000 Hz anti-aliasing filter. The data were processed according to SAE J211 with a CFC 600 filter. The peak forces and moments along each axis and in each direction were determined from the data, along with the corresponding times relative to the initiation of the deceleration pulse.

The relative stiffness of the seat backs of the standard production and all-belts-to-seats systems was determined through an analysis of seat back angle extracted from the high speed video and compared for tests with 2.2 and 5.4 m/s delta V. Because impacts were repeated at the 2.2 and 5.4 m/s delta V levels, the repeatability of sled impact pulses was assessed by calculating the linear correlation coefficient ( $r$ ) of the time course of delta V at both impact speeds.

## RESULTS

### KINEMATICS AND KINETICS OF THE LUMBAR SPINE

For our analysis, we defined two general phases of ATD motion: (1) a “ramping” phase in which the ATD moves backward relative to the seat bottom, with lumbar spine generally in extension and (2) a “rebounding” phase in which ATD moves forward relative to seat bottom, with the lumbar spine generally in flexion. The “rebounding” phase starts at the end of the “ramping” phase, continues through maximum flexion and ends with the ATD generally its initial configuration. Throughout the tests, the largest components of force and moment were in the sagittal plane.

During the “ramping” phase, the ATDs began in normal seated positions (Figures 3A and 4A) and experienced a forward-directed acceleration as the sled decelerated. The high-speed video showed that the ATD torso moved backward relative to the pelvis during this phase. The relative accelerations between the ATD and the seat caused the body of the ATD to move backward and upward along the angled, backward-flexing seat back. Because the lap portion of the restraint system restrained the pelvis and femoral regions, the ATD kinematics of the upper body resulted in a combination of axial tension-extension in the lumbar spine. The upward ramping motion of the ATD torsos along the seat back was arrested by the lap belt restraint, causing tensile forces to be exerted on the lumbar spine (Figures 3B and 4B).

During the “ramping” phase, the Hybrid III ATD displayed an initial negative (compression) peak prior to the development of the axial tensile force (arrow, Figure 5). This result was observed in all of the rear impact tests using the Hybrid III. The BioRID II, in contrast, did not always display an initial compressive force preceding the tensile force. Initial backward motion was more exaggerated in the standard bucket seats of the Ford Taurus than in the all-belts-to-seats system used in the Chevrolet Suburban.

The “rebound” phase started with the ATD in maximum extension. During the “ramping” phase, the seatbacks were loaded and energy was stored elastically. This elastic energy was restored to the ATD body during the “rebound” phase. During this “rebound” phase, the body of the ATD moved down the seat back and transitioned from extension into flexion. The articulating segments in the BioRID II spinal structure allowed the BioRID to flex forward further and for a longer duration when compared to the more rigid spine of the Hybrid III. However, flexion in both ATDs was quickly arrested by the shoulder belt of the restraint before significant amounts of flexion were achieved (Figures 3C and 4C). Finally, the ATD body oscillated to a final equilibrium near its initial configuration (Figures 3D and 4D). This final

motion was more damped in the Hybrid III than in the BioRID II.

<figure 3 here>

<figure 4 here>

<figure 5 here>

### COMPARISON OF BIORID II AND HYBRID III RESPONSES

The Hybrid III generally experienced higher reaction forces in the lower lumbar spine than the BioRID II for Tests A-D (Figure 5). Specifically, compressive loads and bending moments were higher in the Hybrid III at all impact speeds tested. The highest compressive load ( $F_z$ ) of 0.87 kN was observed in the Hybrid III during the 3.6 m/s (8 mph) impact at 98 ms; this peak force was 2-fold higher than in the BioRID II. At the point in time where the peak compressive force was a maximum for the Hybrid III, the peak moment was essentially zero ( $M_y = -0.0003$  kN·m). The peak extension moment in the Hybrid III occurred at 161 ms and was 0.14 kN·m, nearly 3 times higher than that observed in the BioRID (0.05 kN·m). The peak flexion moment was 0.09 kN·m in the Hybrid III, which was 65% higher than in the BioRID (0.05 kN·m). The peak shear load ( $F_x$ ) of 1.28 kN was also observed in the Hybrid III during forward motion, and this was almost 6 times higher than in the BioRID II.

In contrast, the BioRID II sustained slightly higher rearward-directed shear loads than the Hybrid III. The peak positive shear was 0.60 kN and 0.40 kN in the BioRID II and Hybrid III, respectively, a difference of 50%. Both ATDs sustained comparable tensile loads; the peak tensile load was 1.70 kN and 1.46 kN in the BioRID II and Hybrid III, respectively, a difference of only 16%. Lower lumbar loads in both ATDs generally increased with impact severity.

COMPARISON OF SEAT TYPES Sled impact pulses varied minimally between impacts with standard production seats and those with all-belts-to-seats systems ( $r = 0.9999$  for 5 mph;  $r = 0.9997$  for 12 mph).

Extension during the “ramping” phase was more pronounced with standard seats when compared to the all-belts-to-seats systems, suggesting that the all-belts-to-seats system was stiffer. This was further evidenced by the residual damage to the seat back following rear impact tests, where a larger amount of plastic deformation was observed in standard production seats. Analysis of seatback angle from the high-speed video indicated that the all-belts-to-seats system was between 1.6 and 2 times stiffer than standard production seats.

Though the extension was more pronounced for the tests using standard seats, the injury potential of standard seats (Tests A-D) was similar to the all-belts-to-seats (Tests E-F) systems. For all tests, the largest force component in the lumbar spine was axial tension and the axial tension was similar in magnitude between all-belts-to-seats and production seats. The compressive loads were also similar (Figure 7). Finally, the compressive loads in all of the tests did not exceed 0.9 kN. For the tests that used the all-belts-to-seats systems, the peak spinal compressive loads were comparable among similar ATD types in the 5 and 12 mph delta V tests (Figure 6).

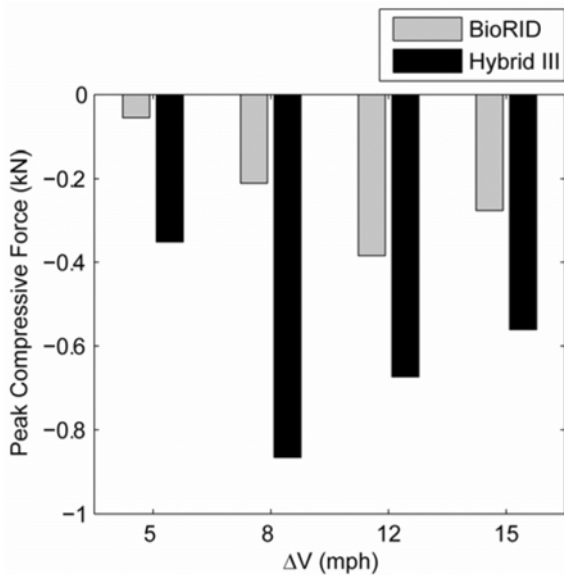


**Figure 6. Peak compressive loads of the lumbar spine (in kN) at 2.2, 3.6, 5.4, 6.7 m/s (5, 8, 12, and 15 mph) delta Vs observed while ATDs were restrained in Ford Taurus seats.**

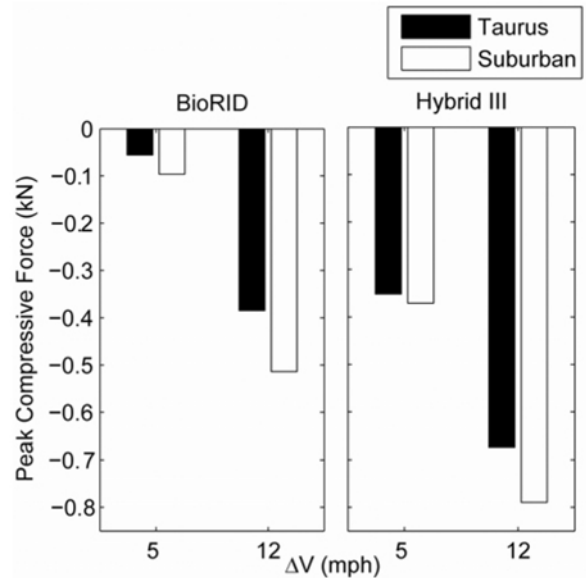


**Figure 7. Peak compressive loads of the lumbar spine for (in kN) at 2.2 and 5.4 m/s (5 and 12 mph) delta Vs for both Ford Taurus and Chevrolet Suburban seats.**

## DISCUSSION

In this study, we examined the responses of a Hybrid III and a BioRID II during simulated rear end crashes. For varying degrees of impact severity, we measured the loads at the lumbar spine and the body segment motions of each ATD using load cells and high-speed cameras. These loads and motions were compared to data from *in vitro* studies that reported the forces and motions required to create lumbar disc herniations. Evidence of traumatic loading conditions would have been in the form of a sudden axially-directed compressive force imposed following a period of significant spinal bending moment. This was not observed in any of the tests with either ATD. Shear forces, while reported for completeness, are effectively resisted by the facet joints in the human spine [11] and are unimportant to this discussion.

## KINEMATICS OF THE LUMBAR SPINE: COMPARISON TO VOLUNTEER AND OTHER ATD STUDIES

Others have recorded the motions of volunteers (live occupants) and ATDs in low-speed, rear end collisions [21,22,23,24]. The results of these studies show that a stationary, off-vehicle observer would see two parts to the relative motion between the seat and the occupant: (1) the seatback moving forward into the occupant during the initial acceleration phase and (2) the occupant rebounding forward off of the seat (toward the front of the vehicle) as the vehicle decelerated. When observed from within the vehicle, these two phases would appear as: (1) the occupant moving rearward into the seatback and (2) the occupant moving

forward off of the seat toward the front of the vehicle. For restrained occupants, the forward torso movement would be limited by the lap and shoulder belt during this second phase. In results the present study showed ATD motions that were qualitatively similar to the volunteers, with similar phases.

The lumbar loads and body segment motions we observed were similar to those described by others in previous studies using ATDs and volunteers. Viano and Olsen (2001) reported the Hybrid III lumbar loads for laboratory simulated rear end crashes using Saab seats with and without the Saab Active Head Restraints (SAHR) system [21]. The Viano and Olsen also used two delta Vs that we used in our study; these were 3.6 and 6.7 m/s delta Vs. For these delta Vs, the lumbar loads measured here were similar to those reported by Viano. The differences between the values measured are likely due to differences in the seats. For example, in our 6.7 m/s tests, the peak extension and flexion moments were 0.14 kN·m and 0.073 kN·m whereas in the Viano tests these values were 0.015 kN·m and 0.042 kN·m for non-SAHR seats and 0.079 kN·m and 0.066 kN·m for SAHR seats.

## INJURY POTENTIAL

Medical personnel routinely find lumbar disc damage, such as a posterior disc herniation, without damage to other structures of the lumbar spine. We examined the potential for developing posterior disc damage (such as a herniation) by comparing the loads found in our tests to those related to disc damage creation as described in the literature. The results of tests show that there are two loading combinations on the lumbar spine during a rear end collision: axial compression-extension and axial tension-flexion.

During the “ramping” phase, the lumbar spine experienced tension and extension. For both ATDs in our tests, axial tension and extension moment were the largest force and moment components during this phase. To our knowledge, no peer-reviewed publication has shown that this loading combination can damage a lumbar disc (that is in physiologic range of motion) without first damaging other structures of the spine. The studies that looked at extension consistently reported posterior bony damage first. For example, Adams et al. conducted an *in vitro* study of lumbar spinal units subjected to extension moments [25]. In this work, the authors found that the facets and the spinous processes were the first structures damaged in extension. Additionally, these authors reported that lumbar disc damage from hyperextension could occur with fatigue loading or when a large compressive load was applied to the vertebra at the same time; the average compressive load at failure was 7,432 N (range: 3,421 to 12,200 N). Because we measured tension during lumbar extension, these conditions were not met during the “ramping” phase of any of our tests. During the “ramping” phase of a rear end collision, the force and moment components acting on an occupant's lumbar spine

would be unlikely to damage the intervertebral disc, unless other structures were damaged first.

During the “rebound” phase, the lumbar spine experienced compression and flexion. For both ATDs in all of our tests, axial compression and flexion moment were largest force and moment components during this phase. There have been many studies conducted on the relationship between lumbar disc herniations and the combination of axial compression and flexion moment [12, 14]. The authors of studies were not able to generate lumbar disc herniations without first damaging the vertebral body (for example, end plate fractures) or the posterior structures of the lumbar spine. In order to produce only disc damage (that is, without damaging other structures) under axial compression and flexion, the experimenters had to remove the posterior elements and introduce hyperflexion to the spinal segment. In this altered configuration, the average compressive force associated with disc damage was 5,448 N (range: 2,760 to 12,968 N). The magnitude of axial compression we measured in our tests (maximum 870 N for the Hybrid III in the 3.6 m/s test) never reached the range associated with damage during any portion of our tests; this was true for both ATDs and for all speeds tested.

Yoganandan et al. studied incremental disc damage that is related to the formation or continued generation of a disc herniation [26]. In this study, the authors found that the mechanical properties of the disc changed at between 2.7 and 10 kN of compressive load. This change in mechanical properties is termed microtrauma. Microtrauma would be coded as AIS 1, while disc herniation would be coded as AIS level 2 (no neural involvement) or AIS level 3 (neural involvement). None of our tests generated loads high enough to enter the microtrauma initiation range found by Yoganandan et al [26].

## COMPARISON OF BIORID II AND HYBRID III LOADS

The results of our tests showed that the axial compressive force was lower for the BioRID II when compared to the Hybrid III ATD during the same tests. The maximum axial compressive force for the Hybrid III was typically at the beginning of the “ramping” phase. One potential reason that the Hybrid III developed an initial compressive force immediately after impact is the angle of the lumbar load cell. In the Hybrid III, the lumbar load cell is tilted posteriorly by 22 degrees. Because of this angle, an anteriorly-directed force pushing on the kyphotic lumbar member of the Hybrid III was found to create some apparent compression.

A numerical evaluation was conducted to address the effect of this angle. It must be understood that the reported values for axial compression/tension ( $F_z$ ) and for anterior/posterior

shear ( $F_x$ ) are different in the two ATDs (see [Figure 5](#)). The Hybrid III's directions for  $F_x$  and  $F_z$  are rotated by 22 degrees about the lateral axis, compared to the analogous directions for the BioRID II (see [Figure 1](#)). The following planar rotation enabled the forces measured by the Hybrid III to be transformed to the coordinate system of the BioRID:

$$F'_x = F_z \sin \theta + F_x \cos \theta$$

$$F'_z = F_z \cos \theta - F_x \sin \theta$$

where  $\theta = 22$  degrees. When applied to the measured force data for Tests C and D, for instance, the initial compressive force peaks of the transformed axial force  $F'_x$  were reduced by about two-thirds ([Figure 8](#)). Less dramatic results were obtained in Tests A and B but, in all cases, the initial compressive force peak was reduced. Therefore, the rearward-sloping mounting platform of the Hybrid III accounts for much, but not all, of the initial negative compressive force observed when using the Hybrid III ATD in rear impact tests.

The curved, stiff (but non-rigid) lumbar segment in the Hybrid III may also contribute to the initial compressive force measured. Forcible backward extension of the lumbar segment causes the kyphotic curvature to straighten and straightening tends to cause the lumbar spine to lengthen in the axial direction. The lumbar spine segment can only lengthen if it pushes the torso and pelvis apart. Because the torso and pelvis have significant inertia, a short-duration initial compressive force could develop.

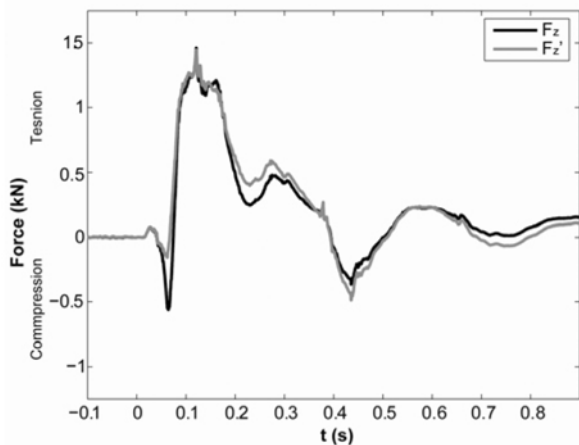


**Figure 8. Lumbar compressive force measured at the lumbar load cell of the Hybrid III ATD, compared to the transformed axial force  $F'_z$  from Test D (delta V = 6.7 m/s or 15 mph). The transformation corrects for much of the initial axial compressive force peak measured using the Hybrid III and does not significantly alter the measured forces thereafter.**

The kyphotically curved lumbar spine segment of the Hybrid III also appears to have affected the shear force and bending moment. An anteriorly-directed force exerted on the lumbar segment results in a negative value of  $F_x$ . Because the apex of the lumbar segment protrudes noticeably rearward, it is likely that this section penetrated into the seatback the furthest, developing a concentrated force that was transmitted directly to the load cell in the form of a negative shear force. It is also thought that the rearward protrusion may have acted as a fulcrum, causing a stronger extension moment to be measured by the load cell in the Hybrid III as compared to the BioRID II.

Small amounts of lumbar spinal bending during the tests were not directly observable in the high-speed videos. At the time of peak spinal compression load, the bending moments were uniformly low (less than 39 N-m; see [Table 2](#)). The peak bending moments were reached well after the apparent spinal compression forces had reached their peak values. It can therefore be argued that significant spinal bending could not have developed at the time of the peak compression forces due to lack of both significant bending moments and time required to develop segmental angular rotations.

Other reasons for the presence of initial compression in the Hybrid III data, and its absence from the BioRID II data (see [Table 3](#)), include variances produced by the stiff Hybrid III torso versus the multiple-linked flexible spine of the BioRID II, as well as the backward leaning angles of the pelvis and torso in the initial positioning of the ATDs. In the latter case, it is possible that the ability of the BioRID II to better conform to the seatback contours reduced the backward leaning angles of its instrumentation. The Hybrid III, on the other hand, could have significant leverage exerted at the lumbar load cell by a distant force, causing bending of the lumbar member and the imposition of an apparent compressive force and bending moment. Whether this occurs in a live human is dependent upon the inclination angle of the pelvis, the configuration of the lower seatback and lumbar support, and the posture of the human subject. However, no evidence of significant spinal bending and simultaneous spinal compression was observed in the current series of tests.

The Hybrid III data set is expanded to include additional rear impacts up to 9.3 m/s (20.7 mph) delta V (see [Appendix A](#)). That Hybrid III data followed similar trends to the current results presented herein. An initial spinal compressive force was observed that remained less than 0.825 kN, followed by the development of a tensile force.

<[table 2](#) here>

<[table 3](#) here>

## CONCLUSION

Initial lumbar compression recorded by Hybrid III ATDs are likely due to the kyphotic curvature of the lumbar spine segment and the posteriorly-sloped lumbar load cell mounting surface. In normal circumstances, with seats and seatbacks in good condition and an occupant in a normal seated position, rear impact automobile collisions with delta Vs up to 9.3 m/s (20.7 mph) do not produce much, if any, lumbar axial compression. Because the lumbar axial compression was small and significant axial compression is required to create damage to the intervertebral disc, it is unlikely that low to moderate speed impacts could cause significant damage to the lumbar discs.

## ACKNOWLEDGEMENTS

The authors wish to acknowledge the support of Exponent Failure Analysis Associates in the development of this paper. The authors would also like to recognize Ryan Hoover for his assistance in data processing.

## REFERENCES

1. Banks, R., Martinin, J., Smith, H., Bowles, A., McNish, T., and Howard, R., "Alignment of the lumbar vertebrae in a driving posture," *Traffic Injury Prevention*, 2(2): 123-130, 2000.
2. Hildingsson, C. and Toolanen, G., "Outcome after soft tissue injury of the cervical spine: A prospective study of 93 car accident victims," *Acta Orthopædica Scand*, 61(4): 357-359, 1990.
3. Kakis, F. and Ripsom, G., "Mechanisms of injury: Understanding the physics of low energy rear-end collisions," *Claims*: 41-46, 1996.
4. Stapp, J., "Historical review of impact injury and protection research", in *Impact Injury of the Head and Spine*, Ewing C., et al., Editors: Springfield. p. 5-40, 1983.
5. Nielsen, G., Gough, J.P., Little, D.M., West, D.H., and Baker, V.T., "Low speed rear impact test summary - Human test subjects," *Accident Reconstruction Journal*, Sept/Oct: 40-43, 1996.
6. Adams, M. and Hutton, W., "The relevance of torsion to the mechanical derangement of the lumbar spine," *Spine*, 6(3): 241-248, 1981.
7. Adams, M.A. and Hutton, W.C., "The effect of fatigue on the lumbar intervertebral disc," *Journal of Bone and Joint Surgery*, 65-B(2): 199-203, 1983.
8. Kapandji, I.A., "The Physiology of the Joints, Second Edition": Churchill Livingstone, New York. 1974.
9. White, A.A. and Panjabi, M.M., "Clinical Biomechanics of the Spine". 2 ed: J.B. Lippincott Co., Philadelphia. 1990.
10. Adams, M. and Hutton, W., "The mechanics of prolapsed intervertebral disc," *International Orthopaedics* 6: 249-253, 1982.
11. Adams, M.A. and Hutton, W.C., "The mechanical function of the lumbar apophyseal joints," *Spine*, 8(3): 327-330, 1983.
12. Adams, M.A. and Hutton, W.C., "Prolapsed intervertebral disc - A hyperflexion injury," *Spine*, 7(3): 184-191, 1982.
13. Hickey, D.S. and Hukins, D.W.L., "Relation between the structure of the annulus fibrosus and the function and failure of the intervertebral disc," *Spine*, 5(2): 106-116, 1980.
14. Brinckmann, P., "Injury to the annulus fibrosus and disc protrusions - An in vitro investigation on human lumbar discs," *Spine*, 11(2): 149-153, 1986.
15. Davidsson, J., "Human volunteer kinematics in rear-end sled collisions", Chalmers University of Technology: Göteborg, 1999.
16. Davidsson, J., Lovsund, P., Ono, K., Svensson, M.Y., and Inami, S., "A comparison between volunteer, BioRID P3 and Hybrid III performance in rear impacts", in *IRCOBI Sitges*: Spain. p. 165-178, 1999.
17. Davidsson, J., "BioRID II final report", Chalmers University of Technology: Göteborg, 1999.
18. Inman, V.T., Ralston, H.J., and Todd, F., "Human Walking": Williams & Wilkins, Los Angeles. 1981.
19. "User's Manual for the 50th Percentile Male Hybrid III Test Dummy," SAE International Engineering Aid (EA-23), Warrendale, PA, 1998.
20. Welch, T., Bridges, A., Gates, D., Heller, M. et al., "An Evaluation of the BioRID II and Hybrid III during Low- and Moderate-Speed Rear Impact," SAE Technical Paper [2010-01-1031](#), 2010.
21. Viano, D.C. and Olsen, S., "The effectiveness of active head restraint in preventing whiplash," *J Trauma*, 51(5): 959-969, 2001.
22. Szabo, T.J., Welcher, J.B., Anderson, R.D., Rice, M.M. et al., "Human Occupant Kinematic Response to Low Speed Rear-End Impacts," SAE Technical Paper [940532](#), 1994.
23. McConnell, W.E., Howard, R.P., Guzman, H.M., Bomar, J.B. et al., "Analysis of Human Test Subject Kinematic Responses to Low Velocity Rear End Impacts," SAE Technical Paper [930889](#), 1993.
24. West, D.H., Gough, J.P., and Harper, G.T.K., "Low speed rear-end collision testing using human subjects," *Accident Reconstruction Journal*, 5(3): 22-26, 1993.
25. Adams, M.A., Dolan, P., and Hutton, W.C., "The lumbar spine in backward bending," *Spine*, 13(9): 1-8, 1988.
26. Yoganandan, N., Maiman, D.J., Pintar, F., Ray, G., Myklebust, J.B., Sances, A., and Larson, S.J., "Microtrauma

in the lumbar spine: A cause of low back pain,”  
*Neurosurgery*, 23(2): 162-168, 1988.

## APPENDIX A

Additional testing was performed to test lumbar loads in a Hybrid III ATD using a triaxial load cell to measure forces in compression ( $F_z$ ), flexion/extension ( $F_x$ ), and flexion/extension moments ( $M_y$ ). In this test series, the driver's seat from a 2002 Lincoln LS was mounted to the sled facing in a rearward direction. The vehicle seatbelt restraint system and corresponding anchor points matched the dimensions of the vehicle. The seatbelts consisted of a three-point continuous loop system. These seats were tested at delta Vs of 7.3 and 9.3 m/s (16.4 and 20.7 mph). A 50<sup>th</sup>-percentile Hybrid III was placed in the driver's seat and secured with a three-point harness system, in accordance with FMVSS 208 (Figure A-1). The BioRID II is not rated for delta V's of this range and was not tested.

Results from these tests appeared to be similar to the results presented for 2.2 to 6.7 m/s (5 to 15 mph) delta V impacts, and extend the results obtained with the Hybrid III ATD to 9.3 m/s (20.7 mph) (Figure A-2). The peak compressive forces measured at the lumbar load cell were 825 N and 699 N in the 7.3 m/s (17 mph) and 9.3 m/s (21 mph) delta V tests, respectively.



**Figure A-1.** Test set-up for the Lincoln rear impact tests. A Hybrid-III ATD was seated in the driver's seat mounted rigidly to the pneumatic sled used in the tests previously described. Tests delivered approximately 7.3 and 9.3 m/s (17 and 21 mph) delta Vs.

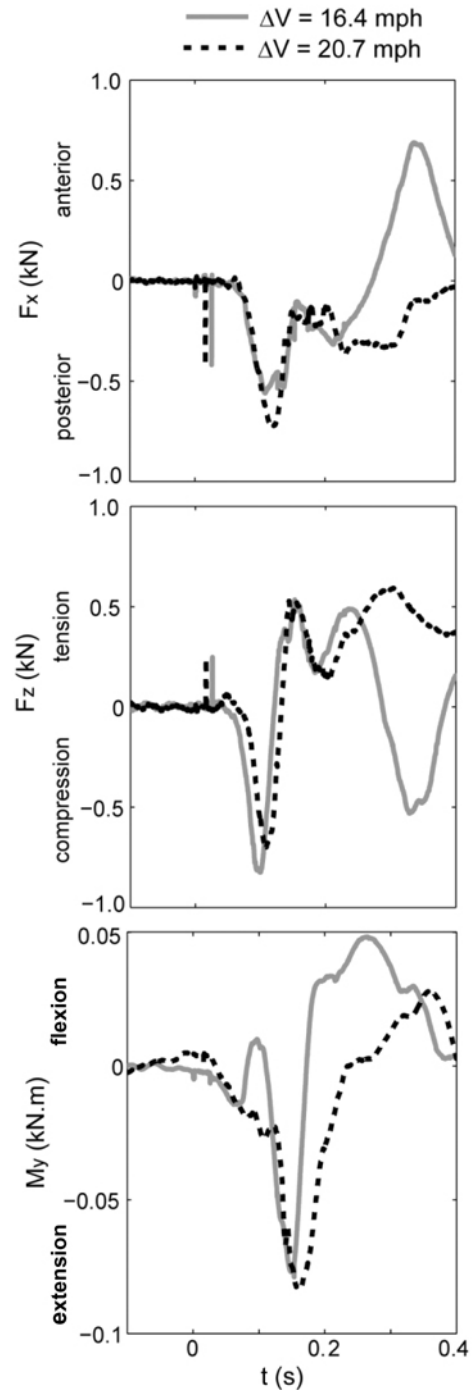


**Figure A-2.** Lumbar loads from the Lincoln LS rear impact tests. The shear force ( $F_x$ ), axial force ( $F_z$ ), and flexion/extension bending moment ( $M_y$ ) were initially negative, similar to the 2.2 to 6.7 m/s (5 to 15 mph) delta V tests described earlier.

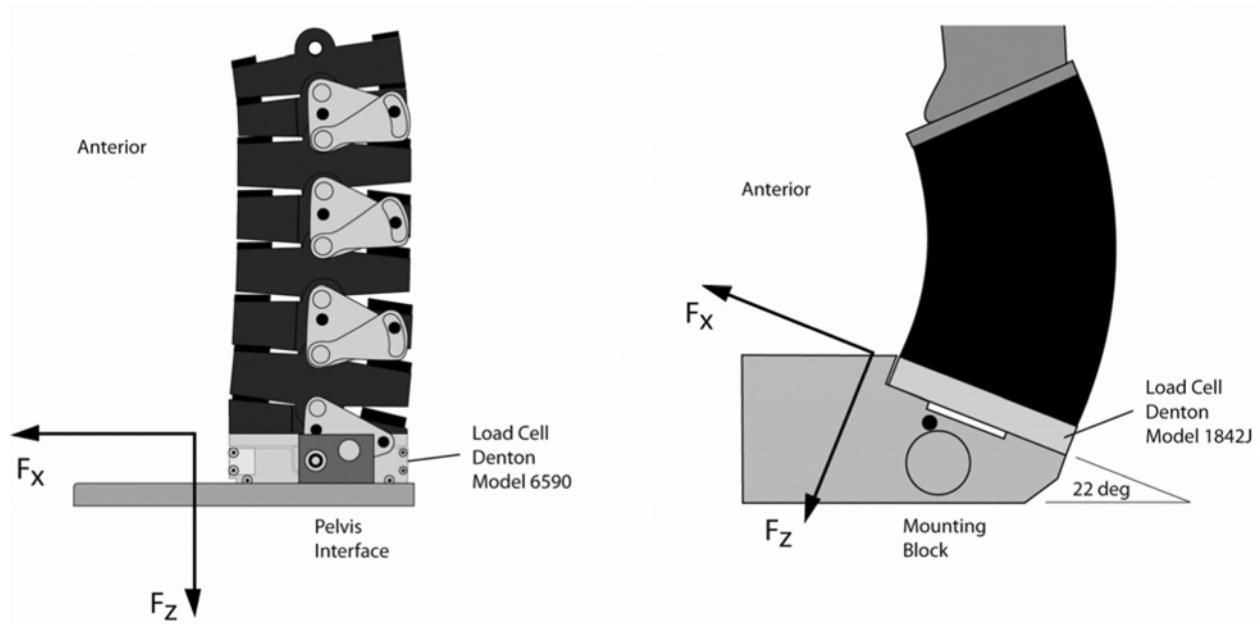


**Figure 1. Schematic diagrams of the BioRID II (left) and Hybrid III (right) lumbar spines, showing the directions of force measurement for shear ( $F_x$ ) and axial loading ( $F_z$ ). The BioRID II attaches to a modified Hybrid III pelvis via a horizontal base plate called the pelvis interface. The Hybrid III uses a mounting block with its posterior surface inclined at 22 degrees posteriorly to mount the load cell. The directions that  $F_x$  and  $F_z$  are measured are therefore different between the BioRID II and Hybrid III.**

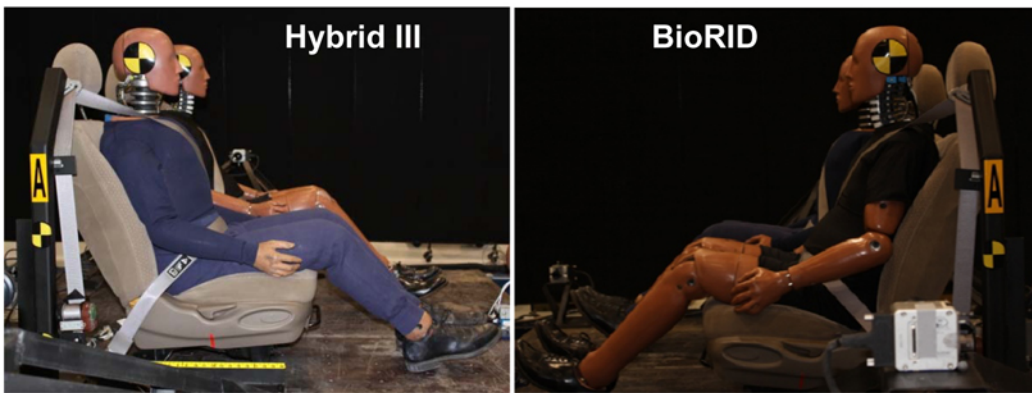
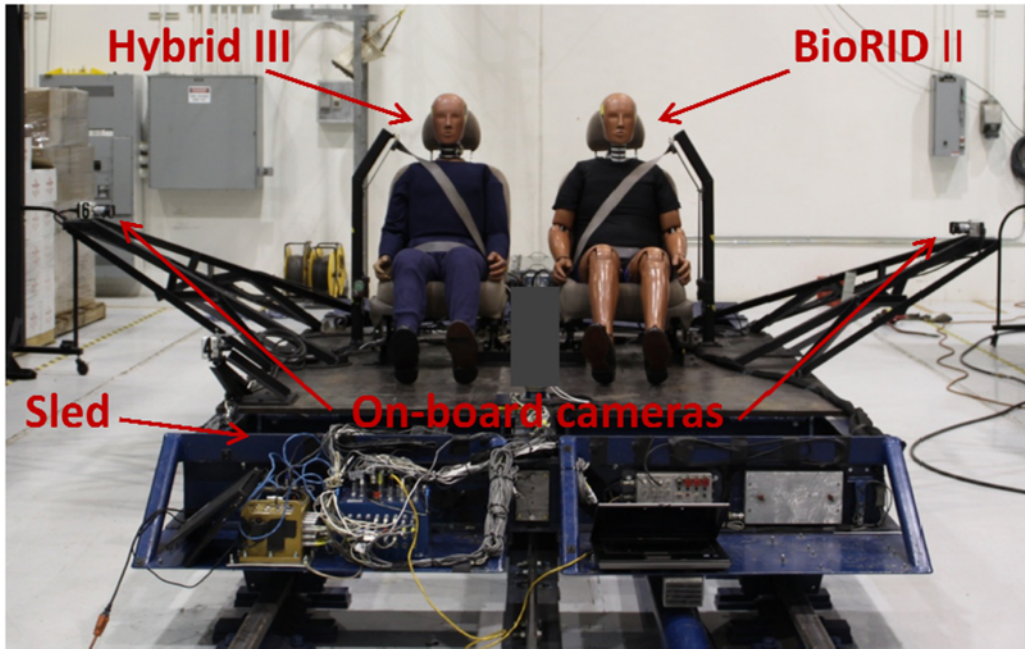


*Figure 2. Test configuration for all tests. A 50<sup>th</sup>-percentile male Hybrid III ATD was placed in the passenger's seat and a BioRID II dummy was placed in the driver's seat. Two on-board cameras monitored the movements of the dummies during testing.*

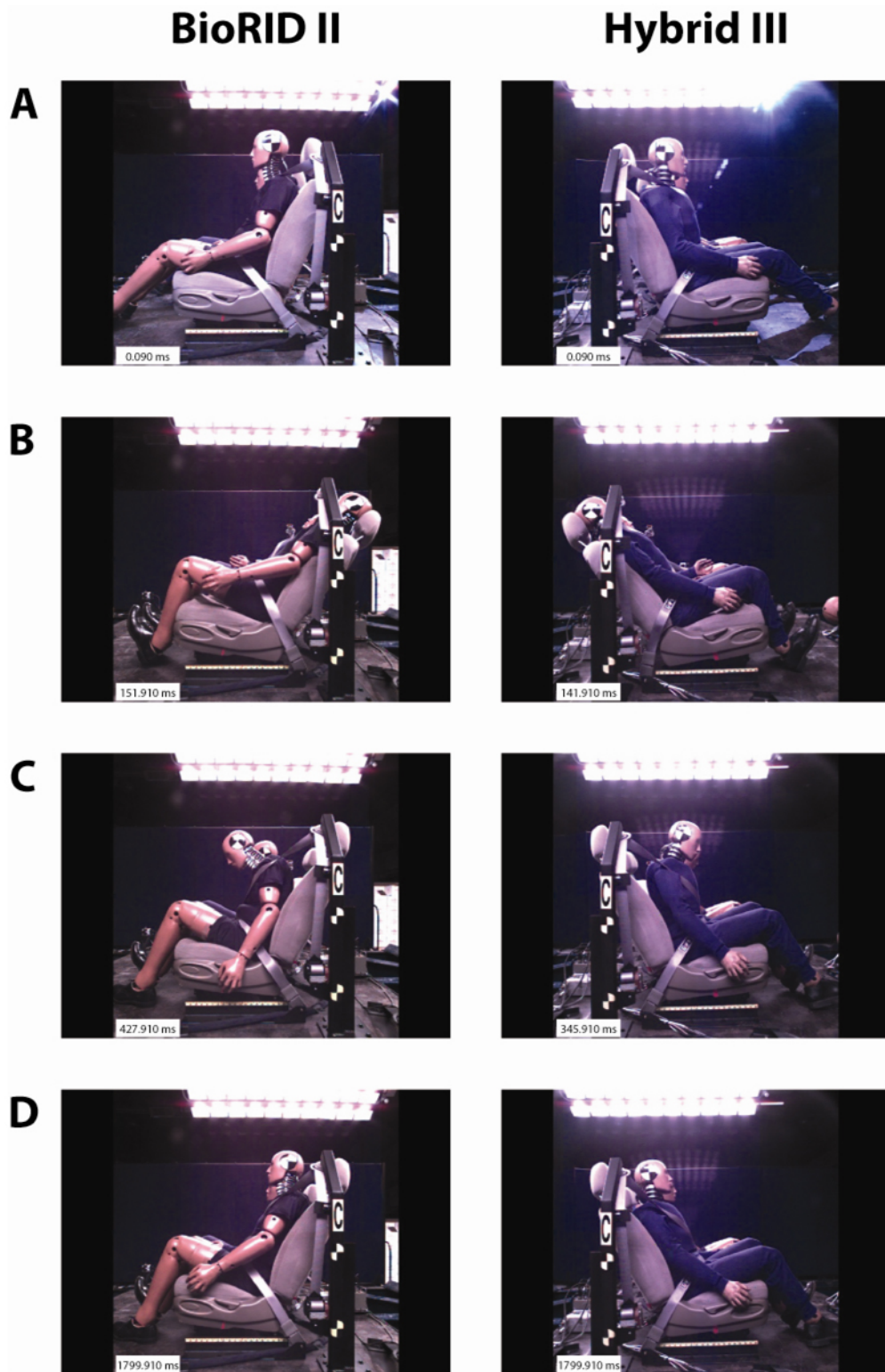


*Figure 3. Kinematics of ATD response to rear impact in standard production seats. Frame captures from video footage of Test C are presented for BioRID II and Hybrid III during 4 phases of the ATD response: A) initial configuration; B) maximum hip extension; C) maximum hip flexion; D) final equilibrium.*

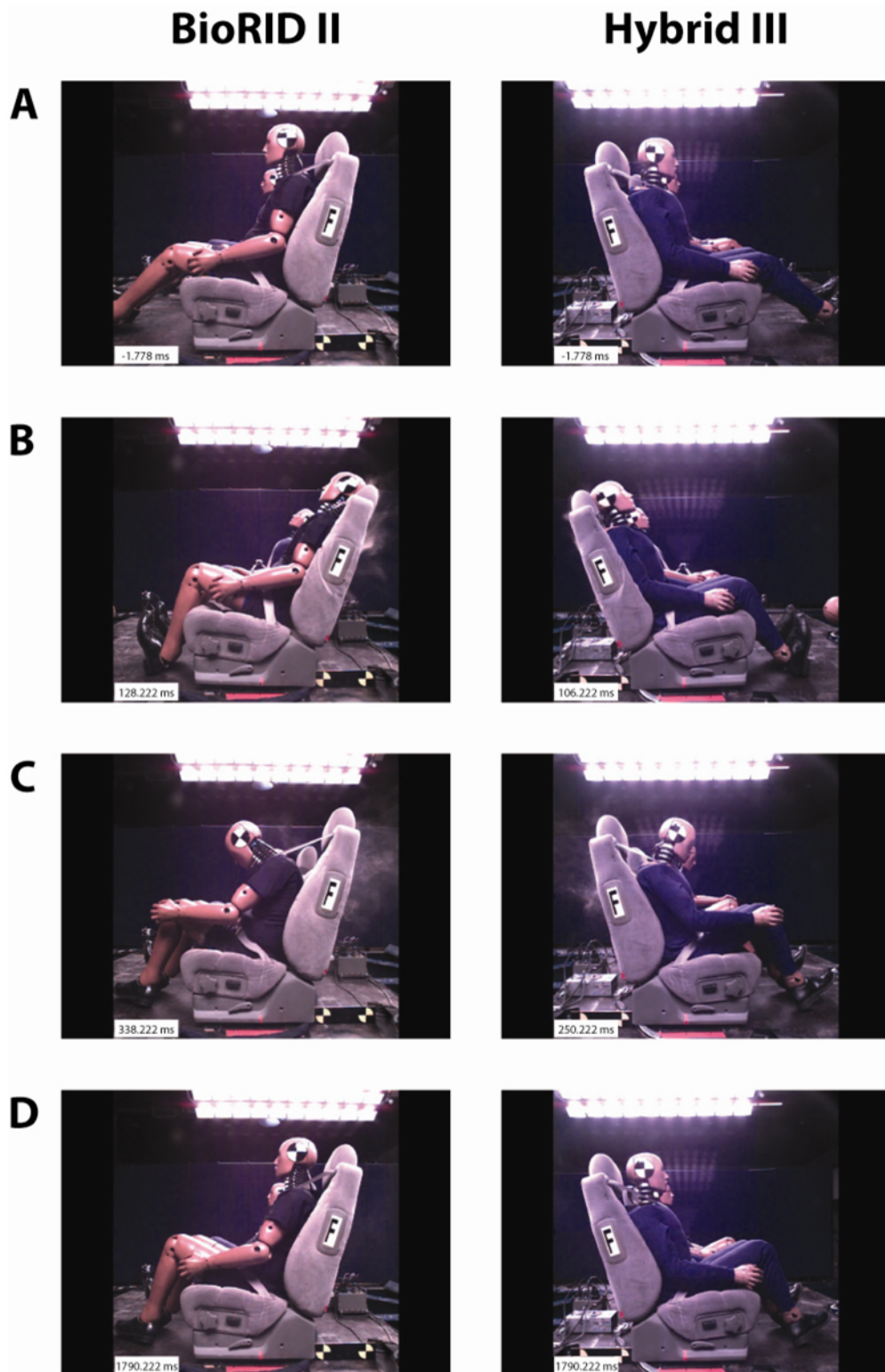


*Figure 4. Kinematics of ATD response to rear impact in all-belts-to-seats. Frame captures from video footage of Test F are presented for BioRID II and Hybrid III during 4 phases of the ATD response: A) initial configuration; B) maximum hip extension; C) maximum hip flexion; D) final equilibrium.*

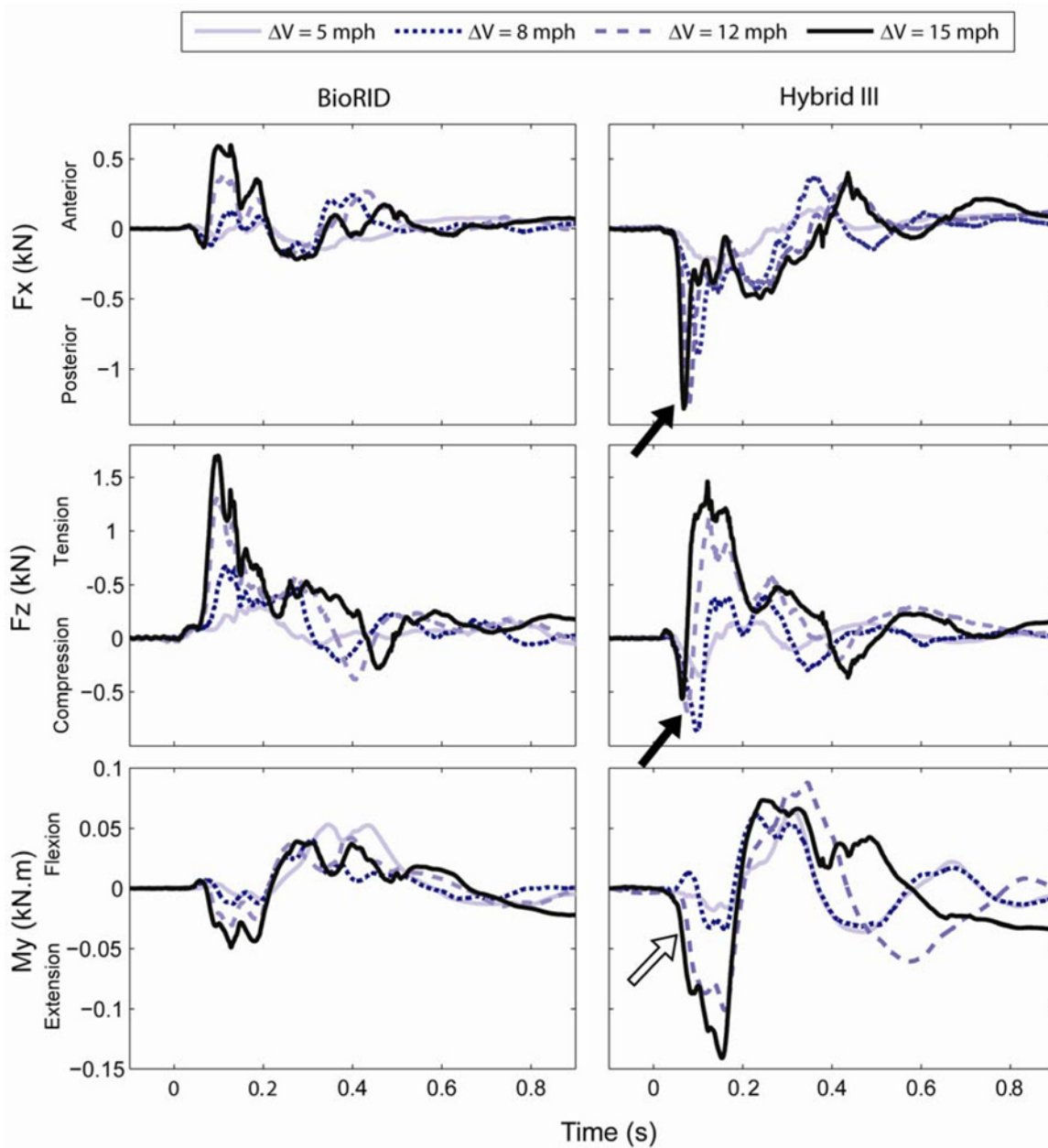


**Figure 5. Lumbar load cell ( $F_x$  and  $F_z$ ) forces and flexion/extension moments ( $M_y$ ) developed during Tests A-D. Note that the Hybrid III developed a posteriorly-directed shear force, a lumbar spinal compressive force, and a large extension moment immediately following the impact. At the time of peak compressive forces (black arrows), the lumbar extension bending moments were still very small (white arrow). This indicates that the amount of spinal bending is likely to be small at the time of maximum axial compression.**

*Table 1. Test Conditions*

<b>Test</b>	<b>Seats</b>	<b><math>\Delta V</math> [m/s (mph)]</b>	<b>Peak acceleration [g]</b>
A	2001-2003 Ford Taurus	2.2 (5)	3.8
B	2001-2003 Ford Taurus	3.6 (8)	5.7
C	2001-2003 Ford Taurus	5.4 (12)	8.5
D	2001-2003 Ford Taurus	6.7 (15)	10.7
E	2001 Chevrolet Suburban	2.2 (5)	3.8
F	2001 Chevrolet Suburban	5.4 (12)	8.4

*Table 2. Lumbar loads measured using the Hybrid III ATD*

<b>Impact Speed [m/s (mph)]</b>	<b>Peak Compressive Load [kN]</b>	<b>Time of Peak Compressive Load [msec]</b>	<b>Bending Moment at Time of Peak Compressive Load [kN·m]</b>	<b>Peak Extension Moment [kN·m]</b>	<b>Time of Peak Extension Moment [msec]</b>	<b>Peak Flexion Moment [kN·m]</b>	<b>Time of Peak Flexion Moment [msec]</b>
2.2 (5)	0.35	102	0.008	0.036	470	0.065	312
3.6 (8)	0.87	98	0.000	0.034	161	0.061	232
5.4 (12)	0.67	75	0.030	0.101	160	0.088	345
6.7 (15)	0.56	64	0.039	0.140	153	0.073	246

*Table 3. Lumbar loads measured using the BioRID II ATD*

<b>Impact Speed [m/s (mph)]</b>	<b>Peak Compressive Load [kN]</b>	<b>Time of Peak Compressive Load [msec]</b>	<b>Bending Moment at Time of Peak Compressive Load [kN·m]</b>	<b>Peak Extension Moment [kN·m]</b>	<b>Time of Peak Extension Moment [msec]</b>	<b>Peak Flexion Moment [kN·m]</b>	<b>Time of Peak Flexion Moment [msec]</b>
2.2 (5)	0.056	333	0.050	0.014	777	0.053	345
3.6 (8)	0.210	370	0.021	0.013	133	0.040	309
5.4 (12)	0.384	407	0.039	0.031	130	0.043	384
6.7 (15)	0.276	455	0.017	0.049	128	0.039	274

---

The Engineering Meetings Board has approved this paper for publication. It has successfully completed SAE's peer review process under the supervision of the session organizer. This process requires a minimum of three (3) reviews by industry experts.

All rights reserved. No part of this publication may be reproduced, stored in a retrieval system, or transmitted, in any form or by any means, electronic, mechanical, photocopying, recording, or otherwise, without the prior written permission of SAE.

ISSN 0148-7191

doi:[10.4271/2010-01-0141](https://doi.org/10.4271/2010-01-0141)

Positions and opinions advanced in this paper are those of the author(s) and not necessarily those of SAE. The author is solely responsible for the content of the paper.

**SAE Customer Service:**

Tel: 877-606-7323 (inside USA and Canada)

Tel: 724-776-4970 (outside USA)

Fax: 724-776-0790

Email: [CustomerService@sae.org](mailto:CustomerService@sae.org)

SAE Web Address: <http://www.sae.org>

Printed in USA

**SAE**International™